

# THERMAL MODEL INTERPRETATION OF PARTICLE PRODUCTION IN $pp$ INTERACTIONS AROUND $s^{1/2} \simeq 10$ GeV

TOMASZ MATULEWICZ, KRZYSZTOF PIASECKI

Institute of Experimental Physics, Faculty of Physics, University of Warsaw  
Warsaw, Poland

*Received 5 December 2023, accepted 13 December 2023,  
published online 20 December 2023*

The statistical hadronization model `ThermalFist` was applied to numerous hadron yields measured in  $p+p$  collisions at  $\sqrt{s} = 8.8, 12.3,$  and  $17.3$  GeV, including recently published yields of  $\phi$  and  $K_S^0$ -mesons, measured by the NA61/SHINE Collaboration. We consistently used the energy-dependent widths of Breit–Wigner mass distributions of hadronic resonances. The canonical treatment of particles with open strangeness combined with the grand canonical approach for non-strange particles gave a moderately reasonable agreement with the measured yields, quantified by  $\chi^2/\text{NDF} \approx 2\text{--}7$ , only when the volume of strange particles was allowed to vary freely. This volume is found to be greater than the one for non-strange matter for all the studied energies. The predicted yields of some of not yet measured particles are provided.

DOI:10.5506/APhysPolB.54.12-A1

## 1. Introduction

For over three decades the predictions of the statistical hadronization models have been compared to the yields of hadrons emitted from heavy-ion ( $AA$ ) collisions, leading to the very successful description of experimental results. A spectacular example is the precise description within the Grand Canonical Ensemble (GCE) of Pb+Pb collisions at the LHC [1], covering 9 orders of magnitude in multiplicity of produced particles at midrapidity. To some surprise, the statistical hadronization model also describes quite well elementary interactions like proton–proton ( $pp$ ) collisions [2–5]. With much lower particle multiplicities in  $pp$  interactions compared to  $AA$ , the conservation of the relevant physical quantities should be applied more strictly than just on average over events. In particular, strangeness is found to be rarely produced in the beam energy range from SIS18 up to SPS. A special treatment of strangeness is usually applied via: (i) reduction of yields

of hadrons containing (anti-)strange quarks, parameterized by factor  $\gamma_S$ , *(ii)* strangeness-canonical approach (SC) combining the canonical treatment of strange hadrons and GCE for the rest of matter, supplemented by *(iii)* a possibility of different volume occupied by strangeness compared to the non-strange bulk [6]. Other improvements to the hadron resonance gas models are considered (for a discussion, see [7]).

Our first statistical model comparison of yields from  $p+p$  at  $\sqrt{s} = 17.3$  GeV [5] was further corrected after the publication of new experimental results of  $\Xi^0(1530)$  and its antiparticle [8]. The calculations were extended towards lower energies [9],  $\sqrt{s} = 12.3$  and 8.8 GeV, where several strange hadron yields have been measured recently by the NA61/SHINE Collaboration. The initial unexpected result, that the volume occupied by strange particles was found to be larger than that of bulk, was consolidated at all the investigated energies. In the current contribution, we update the calculations for the new experimental yields of  $K_S^0$  [10] and  $\Lambda$ . The detailed list of the experimental particle yields and model predictions is provided in Appendix A.

## 2. Thermal hadronization

The statistical approach to the particle emission is successful in the description of the collisions of heavy nuclei at RHIC and LHC energies, where the Grand Canonical Ensemble (GCE) is applied to the copious production of particles ( $\sim 30000$  in  $\sqrt{s}_{NN} = 5.02$  TeV PbPb collision at the LHC). The values of temperature  $T$  and baryochemical potential  $\mu_B$  obtained from these analyses seem to limit the region occupied by the hadron resonance gas at the chemical freeze-out stage in the phase diagram of strongly interacting matter. In contrast, proton–proton collisions at SPS energies provide much lower multiplicity of charged particles, well below 10 for the bulk and below 1 for strange particles. Therefore, the full GCE approach should be excluded in the case of  $pp$  collisions. The ThermalFIST package [6] offers the possibility to apply the Canonical Ensemble (CE) treatment of strange particles while keeping GCE for the remaining particles (the charm production does not play any significant role at these energies). This mixed approach is named SC (Strangeness-Canonical). Applying the CE variant to all the measured species, which ensures the exact conservation of baryon number ( $B = 2$ ) and charge ( $Q = 2$ ), is certainly more restrictive. In the analyses performed so far, the CE approach of the hadron resonance gas turned out not to be very successful in describing particle yields from  $pp$  interactions, as the minimized  $\chi^2$  values are largely above the number of degrees of freedom. Therefore, the results presented here are obtained within the SC variant of the statistical hadronization model.

An improved treatment of broad resonances close to the energy threshold is implemented in **ThermalFIST** through the energy-dependent Breit–Wigner scheme (eBW). We found this recipe [11] reducing slightly the  $\chi^2$  values in most cases and, consequently, use it for all the presented results. Inclusion of eBW resulted in an increase in temperature by about 8 MeV and baryochemical potential by about 10 MeV. The rejection of the yield of  $\phi(1020)$ -mesons performed previously [4] was found to improve significantly the quality of the description of the experimental results. We also observe this effect, however, we decided not to reject any of the experimentally measured particle yields found in a published paper. Following the usual practice, the  $\gamma_S$  undersaturation factor is used to account for the possible non-equilibration of strange particles. In addition, the canonical volume of strange particles is used as a free parameter. The emission volume of strange particles might differ from that of non-strange species and the HBT analyses of kaon pairs from  $pp$  collisions at similar energies were not precise enough to confirm or reject this inequality (see the discussion in [5]). Also in  $AA$  collisions, much better agreement with data was obtained with volumes for strange particles larger than those for the non-strange bulk [12].

### 3. Results and discussion

The results of our calculations within the thermal hadronization model are compared to the experimental yields in Figs. 1–3. The thermal model yield of  $K_S^0$  mesons is evaluated as the average of the yields of  $K_0$  and  $\bar{K}_0$  mesons calculated by the **ThermalFist** code. Our calculations provided the

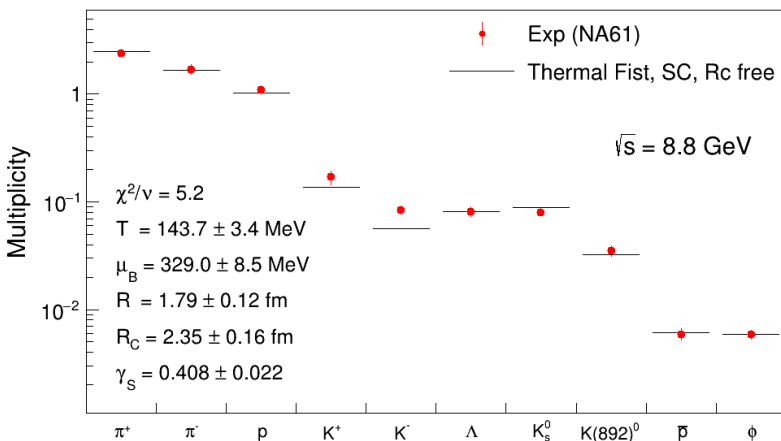


Fig. 1. Results of statistical hadronization model fit (black lines) to the experimental yields (full dots) of hadrons from  $p+p$  at  $\sqrt{s} = 8.8$  GeV.

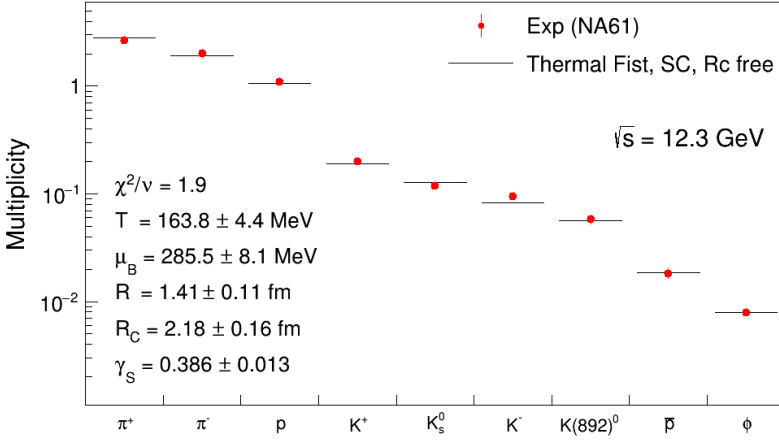


Fig. 2. Results of statistical hadronization model fit (black lines) to the experimental yields (full dots) of hadrons from  $p+p$  at  $\sqrt{s} = 12.3$  GeV.

reasonable values of  $\chi^2/\text{NDF}$  (5.6 at  $\sqrt{s} = 8.8$  GeV, 1.9 at  $\sqrt{s} = 12.3$  GeV, and 6.7 at  $\sqrt{s} = 17.3$  GeV), in contrast to the purely Canonical Ensemble approach or to the scenario with strange particle volume fixed to the bulk ( $\chi^2/\text{NDF}$  values were within 13–26, thus at the level reported in the analysis of NA61/SHINE data [13]). Here, it is worth noticing that in  $AA$  collisions, the  $\chi^2/\text{NDF}$  values are usually found to be  $\sim 1$  for midrapidity yields of hadrons, while significantly higher ( $\sim 10$ ) for integrated ones [14, 15]. The particle yields in  $\sqrt{s} = 8.8$  GeV  $pp$  interaction are described quite well except

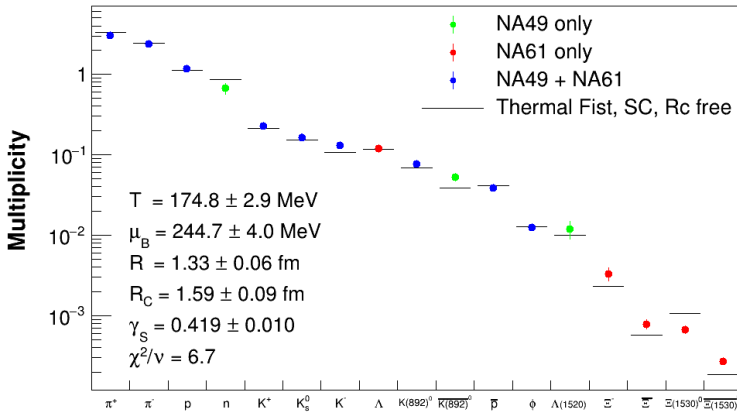


Fig. 3. Results of statistical hadronization model fit (black lines) to the experimental yields (full dots) of hadrons emitted from  $p+p$  at  $\sqrt{s} = 17.3$  GeV.

the case of  $K^-$  meson. Here, the model predictions are significantly below the experimental data. At  $\sqrt{s} = 12.3$  GeV, the agreement with the data is quite good. At both lower energies, the yields of particles were spanning around two orders of magnitude. For completeness, we also show the results for  $\sqrt{s} = 17.3$  GeV [8]. Here (Fig. 3), 17 particle yields span four orders of magnitude. The agreement of predicted yields is again reasonable, with some deviations visible for both  $\Xi(1530)^0$  baryons.

The parameters of best fits to the experimental data are shown in Table 1. With increasing collision energy, we observe the slight increase in temperature and a reduction of the baryochemical potential of the bulk. The strangeness undersaturation factor remains approximately at a constant level of  $\sim 0.4$ . The initial observation at  $\sqrt{s} = 17.3$  GeV, that the radius describing the strangeness canonical volume is larger than that of the bulk, is now seen for all three studied collision energies, at  $3\sigma$  level.

Table 1. Basic parameters of the statistical hadronization model fit to the yields for 3 collision energies of the  $pp$  system. The SC variant of the `ThermalFIST` code was applied, with the radius of strangeness volume allowed to vary freely.

$\sqrt{s}$ [GeV]	8.8	12.3	17.3
$T$ [MeV]	$143.7 \pm 3.4$	$163.7 \pm 4.4$	$174.8 \pm 2.9$
$\mu_B$ [MeV]	$329.0 \pm 8.5$	$285.5 \pm 8.1$	$244.7 \pm 4.0$
$\gamma_S$	$0.408 \pm 0.022$	$0.386 \pm 0.013$	$0.419 \pm 0.010$
$R$ [fm]	$1.79 \pm 0.12$	$1.41 \pm 0.11$	$1.33 \pm 0.06$
$R_C$ [fm]	$2.35 \pm 0.16$	$2.18 \pm 0.16$	$1.59 \pm 0.09$
$\frac{\chi^2}{\text{NDF}}$	$\frac{25.9}{5}$	$\frac{7.6}{4}$	$\frac{80.4}{12}$

The energy dependence of the statistical hadronization parameters is plotted in Fig. 4. Generally, the temperature, baryochemical potential, and strangeness undersaturation factor follow the trend observed in other analyses at energies below  $\sqrt{s} = 20$  GeV. It should be noticed that the uncertainties of the extracted parameters are often smaller compared to the previous analyses, as the number of the experimental yields increased and the precision of these results is often improved. In the case of the analysis presented in [4], three data points are visible at  $\sqrt{s} = 17.3$  GeV. They reflect different analyses: the CE approach was applied separately for NA49 and NA61/SHINE, while the latter dataset was additionally treated with the GCE method. Apparently, for the CE analysis, the deviation between the NA49 and NA61 results far exceeds the uncertainties of each of them. In contrast, our data point at this energy was obtained with all the experimental yields combined, including the recent data and rejecting the unpublished one.

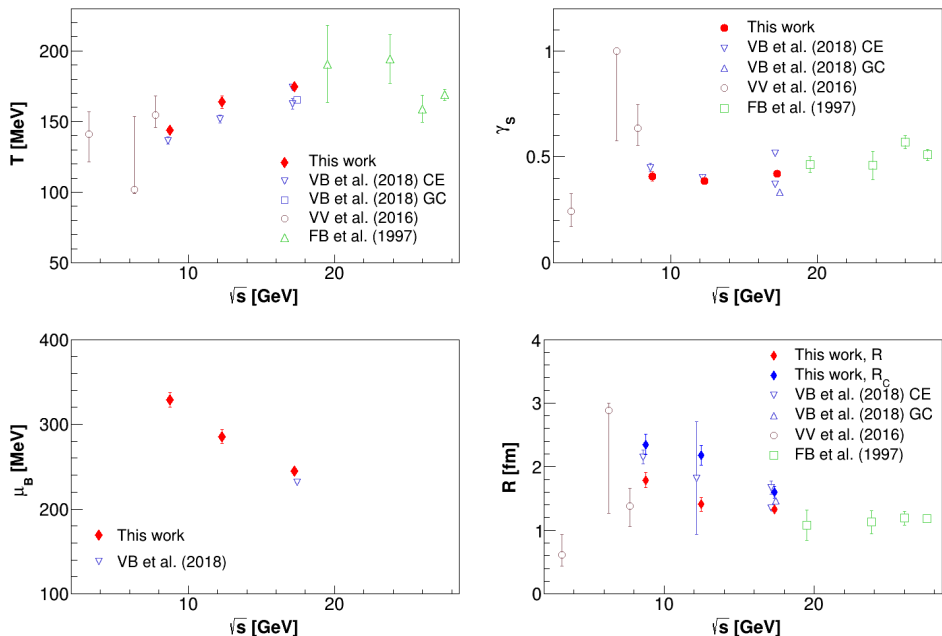


Fig. 4. Energy dependence of basic hadronization parameters: temperature (top left), strangeness undersaturation factor (top right), baryochemical potential (bottom left), and radius of canonical volume (bottom right). The present results are compared to previous analyses: FB refers to [2], VB to [4], and VV to [18]. Note that the current analysis assumes that the volume occupied by the strange hadrons may differ from that occupied by the non-strange matter.

The radius of the bulk volume follows the general trend from other analyses. As mentioned before, the radius of strange particle volume  $R_C$  is found to be significantly larger than that of the bulk. Both radii seem to increase towards lower energies. It might be worth noticing that (within uncertainties) the volume of strange particles appears to be twice as large as that of the bulk.

The relative discrepancy of model calculations  $Y_{\text{stat}}$  with respect to the experimental yields  $Y_{\text{exp}}$ , averaged for all particles measured at three considered energies (36 experimental multiplicities), was found to be

$$\left\langle \frac{Y_{\text{stat}} - Y_{\text{exp}}}{Y_{\text{exp}}} \right\rangle = (-4 \pm 17)\%. \quad (1)$$

This result indicates that the particle yields calculated within the hadron gas model should be considered as a quite good ( $\sim 20\%$ ) prediction of multiplicities of unmeasured particles.

## 4. Conclusions

Numerous yields of particles from  $pp$  interactions (10 species at  $\sqrt{s} = 8.8, 9$  at  $\sqrt{s} = 12.3$  GeV and 17 at  $\sqrt{s} = 17.3$  GeV) were quite successfully reproduced in the hadron resonance gas model implemented in the ThermalFIST code. Some of these yields were recently released by the NA61/SHINE Collaboration. The yields of particles with non-zero net strangeness were treated within the Canonical Ensemble, whereas for the remaining ones, the Grand Canonical approach was applied. The good relative agreement of the hadron gas model calculations with the experimental yields allows to declare an expected  $\sim 20\%$  accuracy of the predicted yields. Those predictions might supplement the transport model calculations with PHSD and PYTHIA 8.2 performed in the broad energy range  $2.7 \text{ GeV} < \sqrt{s_{NN}} < 7 \text{ TeV}$  [16] and in the  $6 \text{ GeV} < \sqrt{s_{NN}} < 25 \text{ GeV}$  range within EPOS 1.99 and UrQMD 3.4 models [17].

The thermodynamic parameters (temperature, baryochemical potential, and strangeness undersaturation factor  $\gamma_S$ ) obtained in this analysis follow the trends observed previously. Their uncertainties are improved compared to many previous analyses. The finding that the canonical volume of strange particles is larger (approximately by factor 2) compared to the bulk is observed also at lower available energies (8.8 and 12.3 GeV). Therefore, this effect calls for experimental (*e.g.* femtoscopy of kaons) and theoretical verification.

The  $pp$  measurements provide an important insight into the thermodynamic properties of  $AA$  collisions. Therefore, extensive  $pp$  measurements at energies comparable to several realized or planned  $AA$  experiments might provide an important reference to those more complex processes.

## Appendix A

### *Particle yields in $pp$ inelastic interactions*

The experimental yields and the results of the thermal hadronization model are presented in this appendix for proton–proton interactions at three available energies of 8.8, 12.3, and 17.3 GeV (beam momentum of 40, 80, and 158 GeV/ $c$ , respectively). The particles listed in the tables are grouped as mesons (non-strange, hidden-strange, open-strange) and baryons ( $|S| = 0, 1, 2$  and 3). The systematic and statistical uncertainties, provided in the original papers, were added in quadrature. The NA49 Collaboration obtained several yields at 17.3 GeV, while the NA61/SHINE contributed at all the considered energies.

The experimental yields listed in Table A.1 and A.2 are taken from [19] except the values for the  $\phi$  [20],  $K^0(892)$  [21] and  $K_S^0$  [10] mesons and  $\Lambda$  baryon only at  $\sqrt{s} = 8.8$  GeV [22].

Table A.1. Experimental particle yields and thermal model calculations within SC approach for  $pp$  interactions at  $\sqrt{s} = 8.8$  GeV.

Particle	Experimental yield	Model
$\pi^0$		2.22
$\pi^+$	$2.39 \pm 0.16$	2.50
$\pi^-$	$1.71 \pm 0.17$	1.68
$\eta$		0.15
$\rho^0(770)$		0.19
$\phi$	$0.00587 \pm 0.00056$ [20]	0.00593
$K_S^0$	$0.080 \pm 0.004$ [10]	0.089
$K^+$	$0.170 \pm 0.025$	0.137
$K^-$	$0.084 \pm 0.007$	0.056
$K^0(892)$	$0.0351 \pm 0.0038$ [21]	0.0321
$\bar{K}^0(892)$		0.0165
$p$	$1.095 \pm 0.090$	1.017
$\bar{p}$	$0.0059 \pm 0.0007$	0.0061
$n$		0.76
$\bar{n}$		0.008
$d$		0.026
$\bar{d}$		$1.6 \times 10^{-6}$
$\Lambda$	$0.082 \pm 0.009$ [22]	0.082
$\bar{\Lambda}$		0.0015
$\Lambda(1520)$		0.005
$\Xi^-$		$1.2 \times 10^{-3}$
$\bar{\Xi}^-$		$0.07 \times 10^{-3}$
$\Xi^0(1530)$		$0.5 \times 10^{-3}$
$\bar{\Xi}^0(1530)$		$0.02 \times 10^{-3}$
$\Omega$		$13 \times 10^{-6}$
$\bar{\Omega}$		$1.7 \times 10^{-6}$

Table A.2. Experimental particle yields and thermal model calculations within SC approach for  $pp$  interactions at  $\sqrt{s} = 12.3$  GeV.

Particle	Experimental yield	Model
$\pi^0$		2.53
$\pi^+$	$2.67 \pm 0.14$	2.77
$\pi^-$	$2.03 \pm 0.17$	1.92
$\eta$		0.22
$\rho^0(770)$		0.24
$\phi$	$0.00789 \pm 0.00041$ [20]	0.00791
$K_S^0$	$0.120 \pm 0.005$ [10]	0.128
$K^+$	$0.201 \pm 0.014$	0.189
$K^-$	$0.095 \pm 0.006$	0.083
$K^0(892)$	$0.0583 \pm 0.0053$ [21]	0.0566
$\bar{K}^0(892)$		0.0029
$p$	$1.093 \pm 0.070$	1.06
$\bar{p}$	$0.0183 \pm 0.0018$	0.0185
$n$		0.79
$\bar{n}$		0.025
$d$		0.027
$\bar{d}$		$14 \times 10^{-6}$
$\Lambda$		0.11
$\bar{\Lambda}$		0.006
$\Lambda(1520)$		0.009
$\Xi^-$		$2.5 \times 10^{-3}$
$\bar{\Xi}^-$		$0.38 \times 10^{-3}$
$\Xi^0(1530)$		$1.1 \times 10^{-3}$
$\bar{\Xi}^0(1530)$		$0.12 \times 10^{-3}$
$\Omega$		$51 \times 10^{-6}$
$\bar{\Omega}$		$17 \times 10^{-6}$

Table A.3. Experimental particle yields and thermal model calculations within SC approach for  $pp$  interactions at  $\sqrt{s} = 17.3$  GeV. The experimental yields newer than those used in [5] are referred explicitly.

Particle	Experimental yield	Model
$\pi^0$		3.14
$\pi^+$	$3.04 \pm 0.17$	3.31
$\pi^-$	$2.40 \pm 0.13$	2.42
$\eta$		0.30
$\rho^0(770)$		0.32
$\phi$	$0.0125 \pm 0.0005$	0.0129
$K_S^0$	$0.162 \pm 0.011$ [25]	0.151
$K^+$	$0.229 \pm 0.016$	0.211
$K^-$	$0.131 \pm 0.008$	0.106
$K^0(892)$	$0.077 \pm 0.006$	0.069
$\bar{K}^0(892)$	$0.052 \pm 0.005$	0.039
$p$	$1.159 \pm 0.033$	1.126
$\bar{p}$	$0.0388 \pm 0.0015$	0.041
$n$	$0.67 \pm 0.10$	0.86
$\bar{n}$		0.053
$d$		0.025
$\bar{d}$		$56 \times 10^{-6}$
$\Lambda$	$0.120 \pm 0.012$	0.118
$\bar{\Lambda}$		0.012
$\Lambda(1520)$	$0.012 \pm 0.003$	0.010
$\Xi^-$	$(3.3 \pm 0.6) \times 10^{-3}$	$2.3 \times 10^{-3}$
$\bar{\Xi}^-$	$(0.79 \pm 0.10) \times 10^{-3}$	$0.58 \times 10^{-3}$
$\Xi^0(1530)$	$(0.673 \pm 0.072) \times 10^{-3}$ [30]	$1.1 \times 10^{-3}$
$\bar{\Xi}^0(1530)$	$(0.271 \pm 0.025) \times 10^{-3}$ [30]	$0.19 \times 10^{-3}$
$\Omega$		$41 \times 10^{-6}$
$\bar{\Omega}$		$22 \times 10^{-6}$

The results available at  $\sqrt{s} = 17.3$  GeV were obtained by both NA49 and NA61/SHINE collaborations. As the NA61/SHINE employs set of TPC detectors inherited from NA49, the systematical uncertainties of experimental results are correlated. The averaging of the results obtained by both collaborations were performed using the method developed by Schmelling [23], as described in [5]. The method is based on the evaluation of the non-diagonal elements of the correlation matrix in such a way that the  $\chi^2$  value equals to the number of degrees of freedom. These averaged values are listed using *italic* in Table A.3. The neutron yield was evaluated (Appendix A in [5]) from the distribution provided by the NA49 Collaboration in [24]. The yield of  $K_S^0$  meson used here is the final result of the NA61/SHINE Collaboration [25]. The uncertainty of this value is factor 4 lower with respect to that obtained by the NA49. Since the latter result was only published as preliminary one in the conference contribution [26], it was abandoned in our dataset. It should be noticed that the expected production of baryons shows rather weak energy dependence (also for multi-strange ones), while the expected production of their antiparticles significantly rises with the collision energy. It is worth to notice that the results at  $\sqrt{s} = 17.3$  GeV are complete as concerning the conservation of electric charge, baryon number, and strangeness (*cf.* Table 2 in [5]). In total, 17 particle yields are measured at this energy, making it a very detailed data set, comparable to that (15 particles) provided at much higher energy of  $\sqrt{s} = 200$  GeV obtained at RHIC [27, 28]. The midrapidity densities of hadrons emitted from the latter collisions have been well described ( $\chi^2/\text{NDF} = 1.1$ ) in the statistical model calculations [29].

## REFERENCES

- [1] A. Andronic, P. Braun-Munzinger, K. Redlich, J. Stachel, «Decoding the phase structure of QCD via particle production at high energy», *Nature* **561**, 321 (2018).
- [2] F. Becattini, U. Heinz, «Thermal hadron production in  $pp$  and  $p\bar{p}$  collisions», *Z. Phys. C* **76**, 269 (1997).
- [3] I. Kraus, J. Cleymans, H. Oeschler, K. Redlich, «Particle production in  $p+p$  collisions at  $\sqrt{s} = 17$  GeV within a statistical model», *Phys. Rev. C* **81**, 024903 (2010).
- [4] V.V. Begun, V. Vovchenko, M.I. Gorenstein, H. Stoecker, «Statistical hadron-gas treatment of systems created in proton-proton interactions at energies available at the CERN Super Proton Synchrotron», *Phys. Rev. C* **98**, 054909 (2018).
- [5] T. Matulewicz, K. Piasecki, «Particle yields in  $pp$  interactions at  $\sqrt{s} = 17.3$  GeV interpreted in the statistical hadronization model», *J. Phys. G: Nucl. Part. Phys.* **48**, 085004 (2021).

- [6] V. Vovchenko, H. Stoecker, «Thermal-FIST: A package for heavy-ion collisions and hadronic equation of state», *Comput. Phys. Commun.* **244**, 295 (2019).
- [7] J. Cleymans, P.M. Lo, K. Redlich, N. Sharma, «Hadronic Resonance Gas Model and Multiplicity Dependence in  $p$ - $p$ ,  $p$ -Pb and Pb-Pb Collisions: Strangeness Enhancement», *Acta Phys. Pol. B Proc. Suppl.* **14**, 435 (2021).
- [8] K. Piasecki, T. Matulewicz, «Statistical hadronization applied to particle yields in  $p+p$  collisions at  $\sqrt{s} = 17.3$  GeV», *PoS (PANIC2021)*, 242 (2022).
- [9] T. Matulewicz, K. Piasecki, «Interpretation of particle yields in  $pp$  interactions at  $\sqrt{s} = 8.8, 12.3$  and  $17.3$  GeV within statistical hadronization model», *EPJ Web Conf.* **276**, 03012 (2023).
- [10] NA61/SHINE Collaboration (H. Adhikary *et al.*), Tech. Rep. «Report from the NA61/SHINE experiment at the CERN SPS», CERN-SPSC-2023-030 SPSC-SR-336, CERN, Geneva, <https://cds.cern.ch/record/2878507>
- [11] V. Vovchenko, M.I. Gorenstein, H. Stoecker, «Finite resonance widths influence the thermal-model description of hadron yields», *Phys. Rev. C* **98**, 034906 (2018).
- [12] J. Cleymans, P.M. Lo, K. Redlich, N. Sharma, «Multiplicity dependence of (multi)strange baryons in the canonical ensemble with phase shift correction», *Phys. Rev. C* **103**, 014904 (2021).
- [13] NA61/SHINE Collaboration (S. Pulawski), «Multi-strange hadron production in  $p+p$  interactions at  $\sqrt{s_{NN}} = 17.3$  GeV», *EPJ Web Conf.* **259**, 11005 (2022).
- [14] F. Becattini *et al.*, «Features of particle multiplicities and strangeness production in central heavy ion collisions between  $1.7 A$  and  $158 A$  GeV/ $c$ », *Phys. Rev. C* **64**, 024901 (2001).
- [15] A. Andronic, P. Braun-Munzinger, J. Stachel, «Hadron production in central nucleus-nucleus collisions at chemical freeze-out», *Nucl. Phys. A* **772**, 167 (2006).
- [16] V. Kireyeu *et al.*, «Hadron production in elementary nucleon-nucleon reactions from low to ultra-relativistic energies», *Eur. Phys. J. A* **56**, 223 (2020).
- [17] MPD Collaboration (K. Shtejer), «Prediction of the particle production in  $pp$  collisions with the MPD detector at NICA collider», *EPJ Web Conf.* **204**, 07005 (2019).
- [18] V. Vovchenko, V.V. Begun, M.I. Gorenstein, «Hadron multiplicities and chemical freeze-out conditions in proton-proton and nucleus-nucleus collisions», *Phys. Rev. C* **93**, 064906 (2016).
- [19] NA61/SHINE Collaboration (A. Aduszkiewicz *et al.*), «Measurements of  $\pi^\pm$ ,  $K^\pm$ ,  $p$  and  $\bar{p}$  spectra in proton-proton interactions at 20, 31, 40, 80 and 158 with the NA61/SHINE spectrometer at the CERN SPS», *Eur. Phys. J. C* **77**, 671 (2017).

- [20] NA61/SHINE Collaboration (A. Aduszkiewicz *et al.*), «Measurement of  $\phi$  meson production in  $p+p$  interactions at 40, 80 and 158 GeV/ $c$  with the NA61/SHINE spectrometer at the CERN SPS», *Eur. Phys. J. C* **80**, 199 (2020).
- [21] NA61/SHINE Collaboration (A. Acharya *et al.*), « $K^*(892)^0$  meson production in inelastic  $p+p$  interactions at 40 and 80 GeV/ $c$  beam momenta measured by NA61/SHINE at the CERN SPS», *Eur. Phys. J. C* **82**, 322 (2022).
- [22] NA61/SHINE Collaboration (H. Ströbele), « $\Lambda$  production in  $p+p$  collisions at 40 and 158 GeV/ $c$ », *J. Phys.: Conf. Ser.* **779**, 012010 (2017).
- [23] M. Schmelling, «Averaging correlated data», *Phys. Scr.* **51**, 676 (1995).
- [24] NA49 Collaboration (T. Anticic *et al.*), «Inclusive production of protons, anti-protons and neutrons in  $p+p$  collisions at 158 GeV/ $c$  beam momentum», *Eur. Phys. J. C* **65**, 9 (2010).
- [25] NA61/SHINE Collaboration (A. Acharya *et al.*), « $K_S^0$  meson production in inelastic  $p+p$  interactions at 158 GeV/ $c$  beam momentum measured by NA61/SHINE at the CERN SPS», *Eur. Phys. J. C* **82**, 96 (2022).
- [26] F. Sikler *et al.*, «Hadron production in nuclear collisions from the NA49 experiment at 158 GeV/ $c \cdot A$ », *Nucl. Phys. A* **661**, 45 (1999).
- [27] B.I. Abelev *et al.*, «Strange particle production in  $p+p$  collisions at  $\sqrt{s_{NN}} = 200$  GeV», *Phys. Rev. C* **75**, 064901 (2007); J. Adams *et al.*, « $\phi$  meson production in Au+Au and  $p+p$  collisions at  $\sqrt{s_{NN}} = 200$  GeV», *Phys. Lett. B* **612**, 181 (2005).
- [28] S.S. Adler *et al.*, «Midrapidity neutral-pion production in proton–proton collisions at  $\sqrt{s_{NN}} = 200$  GeV», *Phys. Rev. Lett.* **91**, 241803 (2003).
- [29] F. Becattini, P. Castorina, A. Milov, H. Satz, «A comparative analysis of statistical hadron production», *Eur. Phys. J. C* **66**, 377 (2010).
- [30] A. Acharya *et al.*, «Measurements of  $\Xi(1530)^0$  and  $\bar{\Xi}(1530)^0$  production in proton–proton interactions at  $\sqrt{s_{NN}} = 17.3$  GeV in the NA61/SHINE experiment», *Eur. Phys. J. C* **81**, 911 (2021).